3 modeling strategies for computing aerated skimming flow parameters over stepped chutes using depth averaged flow solver

S.R. Sabbagh-Yazdi, N.E. Mastorakis, and R. Safaieh

***Abstract*—**In this paper the flow regimes occurring on stepped chutes are reviewed. Then the numerical analysis of skimming flow using a set of depth averaged equations in inclined coordinate system is described. The numerical computations of air entrainment in the skimming flow over stepped spillways are performed using three modeling strategies. In the first modeling strategy, the water flow equations are converted to discrete form using the overlapping cell vertex finite volume method on triangular unstructured mesh, and then, the air concentration distribution is computed using the final solution of flow parameters. In the second modeling strategy, the mean air concentration profiles are computed at every time step of the numerical solution of water flow equations and its effects on reduction of bed friction and flow depth bulking are considered in formation of flow field. In the third modeling strategy, in addition to the second modeling strategy, the effects of changes in air-water mixture on density changes and its effect on flow motion are considered. The computed results of air entrainment into the supercritical skimming flow on stepped spillways are compared with laboratory experimental measurements.

***Keywords*—**Air Concentration, Skimming Flow, Stepped Spillway, Finite Volume Solution, Depth Averaged Equations, Steep Slope

I. Introduction

The advantages of stepped spillways over conventional smooth spillways are excessive air entrainment phenomenon. Air entrainment plays an important role in reducing cavitation risk potential. Stepped spillways provide the important advantage of reducing cavitation risk potential by reducing flow velocities caused by significant air entrainment.

Another advantage is large amount of energy dissipation in comparison with smooth spillways because of the large value of surface roughness. That is why the stepped spillways have gained more attention, particularly with the development of RCC technique in dam construction over the last two decades. Stepped spillways can be easily and economically constructed and attached to the downstream face of RCC dams. They are also used as an overtopping protection system in embankment dams.

As air entrainment is the most important phenomenon which causes the advantages of stepped spillways over conventional smooth spillways, considering the effects of air entrainment in simulating the flow over stepped chutes can help the designers in more accurately determining the geometry of this type of hydraulic structures.

The first author successfully developed a Numerical Analyzer for Scientific and Industrial Requirements (*NASIR*) based on unstructured finite volume method. The version of this software used in this work, solves depth averaged flow equations using cell vertex finite volume method for the explicit solution of the governing equations (Shallow Water Equations modified for steep slopes) on unstructured triangular meshes. The set of equations is solved in horizontal system for subcritical flow (in dam reservoir) and in inclined coordinate system for supercritical flow (over the spillway with steep slope). By multi-layer treatment of the flow field, this version of the software can compute velocity profiles normal to the bed surface [1,2].

In the present work, the results of further development of NASIR finite volume flow solver for considering the effects of air concentration in skimming flow over stepped spillways, are demonstrated. Computer modeling of the air entrainment in the skimming flow over stepped spillways is performed using three strategies. In the first modeling strategy, the water flow parameters are numerically solved, and after the convergence of the solution, the air concentration distribution is computed using the final solution of flow parameters. Therefore, in this strategy the water flow solution results are used by a separate post-processor for computing air concentration. This post-processor uses experimental relations for computing the inception point characteristics and mean air concentration distribution along the stepped chute [3]. In the second modeling strategy, the mean air concentration distribution is computed at every time step of the numerical solution of water flow equations and its effects on reduction of bed friction and flow depth bulking are considered in

Manuscript received March 15, 2008; Revised version received May 17, 2008.

Saeed-Reza Sabbagh-Yazdi is Associate Professor Civil Engineering Department of K.N. Toosi University of Technology, 1346 Valiasr St. Tehran, IRAN (phone: +9821-88521-644; fax: +9821-8877-9476; e-mail: SYazdi@kntu.ac.ir, Web site: http://sahand.kntu.ac.ir/~syazdi/).

Nikos E. Mastorakis, is Professor of Military Institutes of University Education (ASEI) Hellenic Naval Academy, Terma Chatzikyriakou 18539,Piraues, GREECE

Rosita Safaieh is MSc. Graduate of Civil Engineering Department of K.N. Toosi University of Technology, 1346 Valiasr St. Tehran, IRAN

formation of flow field [4]. The third modeling strategy is completed by further development of the second modeling strategy and the effects of the changes in air-water mixture density on flow motion are considered in the two equations of motion [5].

In all of these three modeling strategies the computed mean air concentration is used to plot the air concentration profiles in flow depth using an empirical relation. The air concentration in skimming flow is computed using empirical formulas. While, the flow parameters (i.e. depth and velocity components) are obtained from solution of depth averaged flow equations by unstructured finite volume method. The qualities of the computed results of the three modeling strategies are assessed by comparison with the laboratory measurements reported in the literature [6].

II. Flow Regimes on Stepped Spillways

There are two different flow regimes on stepped chutes: nappe flow and skimming flow.

A. *Nappe Flow*

Nappe flow which happens in low discharges consists of a succession of over-falls jumping from one step to another. The steps act as a series of drops plunged one by one by the falling nappes. One part of energy dissipation in the nappe flow regime occurs when the jet breaks in the air. Another part of energy dissipation is caused by the plunging of nappes on the step surfaces. In this case a series of hydraulic jumps which contributes to energy dissipation might take place.

B. *Skimming Flow*

Skimming flow which happens in large discharges acts as a coherent stream over the outer edges of the steps. These step edges make a pseudo surface over which the flow skims being dissipated by the macro roughness of the steps. The zones formed by the step surfaces and the pseudo bottom contain recirculation vortices which cause part of the energy dissipation in skimming flow regime. The shear transfer from the main stream to the recirculation zone causes the maintenance of the vortices. The exchanges of momentum between the main and the cavity flows results in significant energy dissipation (Fig.1).

A transition flow regime has been observed between the nappe and the skimming flow regimes. At the downstream part of the inception point of air entrainment, transition flow exhibits strong splashing and droplet ejections, and air pockets from small to large sizes can be observed.

In high velocity flows on spillways and steep chutes, the turbulent boundary layer reaches the flow surface at the "point of inception", initiating air entrainment into the flow stream.

Observations have shown that there is a developing flow region after the inception point of air entrainment. For some distance in the developing region, there is a region of partially aerated flow, until the air bubbles penetrate to their maximum depth in the water and the flow becomes fully aerated. After the developing region, there is a fully developed aerated flow region where uniform flow conditions have been obtained.

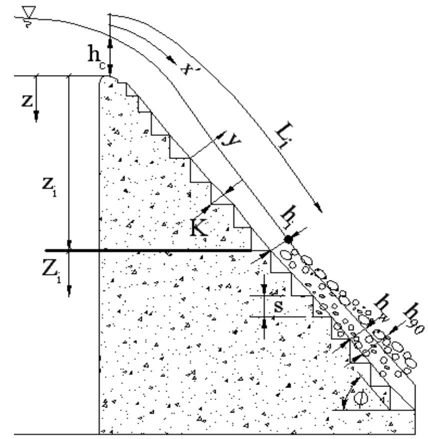

Fig.1: Schematic geometry of the laboratory model and observed flow field [6]

The present work focuses on modeling the skimming flow regime, particularly, computing the flow parameters above the incline surface formed by the step edges. Furthermore, some efforts have been made to consider the effects of air concentration on accurate computation of flow depth and velocity components parallel to the general slope of stepped spillway.

III. Math

In this section, first, the governing partial differential equations of supercritical skimming flow over the stepped spillway and the relation for corresponding bed roughness as well as the relation for producing velocity profile normal to the general surface of stepped spillways are introduced. Then, suggested algebraic relations describing the parameters required for calculating air concentration distribution and its effect on changing flow depth and global friction as well as the relation for producing air concentration profile normal to the general surface of stepped spillways are reviewed.

A. *Flow Equations*

The water phase mathematical equations used in this version of the *NASIR* flow solver are shallow water equations modified for a coordinate system with an axis normal and two axes (x' and y) parallel to the bed surface [1].

$$
\begin{aligned}
&\frac{\partial h'}{\partial t}+\frac{\partial (h'u')}{\partial x'}+\frac{\partial (h'v)}{\partial y}=0\\
&\frac{\partial (h'u')}{\partial t}+\frac{\partial (u'h'u')}{\partial x'}+\frac{\partial (vh'u')}{\partial y}+gh'\frac{\partial \eta}{\partial x'}+\frac{gh'^2}{2\rho_w\cos\alpha}\frac{\partial \rho_m}{\partial x'}\\
&\qquad=-\frac{\tau'_x}{\rho}+\frac{\partial}{\partial x'}\left(\nu_t h'\frac{\partial u'}{\partial x'}\right)+\frac{\partial}{\partial y}\left(\nu_t h'\frac{\partial u'}{\partial y}\right)\\
&\frac{\partial (h'v)}{\partial t}+\frac{\partial (u'h'v)}{\partial x'}+\frac{\partial (vh'v)}{\partial y}+\frac{\partial}{\partial y}\left[h'\frac{gh'/\cos\alpha}{2}\right]+\frac{gh'^2}{2\rho_w\cos\alpha}\frac{\partial \rho_m}{\partial y}\\
&\qquad=-\frac{\tau'_y}{\rho}+\frac{\partial}{\partial x'}\left(\nu_t h'\frac{\partial v}{\partial x'}\right)+\frac{\partial}{\partial y}\left(\nu_t h'\frac{\partial v}{\partial y}\right)
\end{aligned}
\qquad (1)
$$

in which:

$$\frac{\tau_{x'}}{\rho} = c_f u\sqrt{u^2+v^2} \quad ; \quad \frac{\tau_y}{\rho} = c_f v\sqrt{u^2+v^2} \qquad (2)$$

In these equations x' is the axis tangential to the chute slope and y is the same as the y axis in the global coordinate system; u' and v are the velocity components in x' and y directions, respectively; h' is the flow depth perpendicular to the chute bed surface and g is gravity acceleration; α is the chute angle; τ'_x/ρ and τ_y/ρ are the bed surface global stresses in x' and y directions, respectively and $C_f = f_b/4$ is global friction coefficient [2].

In order to use the above described mathematical model for skimming flow over stepped spillway, the effect of the steps has been simulated as bed roughness. For simulating the equivalent bed roughness the following experimental relationship has been used for computing equivalent Darcy Weisbach friction coefficient as [7]:

$$f_b = [0.5 - 0.42\sin(2\phi)]\left(\frac{K}{D_{h,w}}\right)^{0.2} \; ; \quad 19^\circ \le \phi \le 55^\circ \qquad (3)$$

where $D_{h,w}$ is the hydraulic diameter (in terms of clear water depth) and K is the equivalent roughness of the steps.

The depth averaged velocity field parallel to the bed surface that can be computed by solving mathematical model described in aforementioned section, is used for computing the velocity profile in flow depth. Such a velocity profile can be computed using empirical relations suggested for skimming flow over stepped spillways. The relations used for defining velocity profiles in flow depth are as follows[8]:

$$\frac{u}{u_{90}} = 1.05\left(\frac{y}{y_{90}}\right)^{1/4.3} \; ; \; 0.04 \le \frac{y}{y_{90}} \le 0.80$$

$$\frac{u}{u_{90}} = 1 \; ; \frac{y}{y_{90}} > 0.80 \qquad (4)$$

where y_{90} is the characteristic mixture depth with local air concentration of $C=0.90$ and u_{90} is the mixture surface velocity.

B. Air Concentration Relations

The following experimental relations are used for simulating air entrainment. Two empirical relations are proposed in the literature for mean air concentration in fully developed skimming flow over stepped spillways as;

Frizell et al. (2000) [6]:

$$C_{mean} = 0.23 + 0.017\left(\frac{x - L_i}{y_i}\right)^{0.46} \qquad (5)$$

Matos (2000) [9]:

$$\begin{cases} C_{mean} = 0.210 + 0.297\exp\left[-0.497\left(\ln\left(\frac{x-L_i}{y_i}\right) - 2.972\right)^2\right] ; 0 < \frac{x-L_i}{y_i} < 30 \\ C_{mean} = \left[0.888 - \frac{1.065}{\sqrt{\frac{x-L_i}{y_i}}}\right]^2 \qquad ; \frac{x-L_i}{y_i} \ge 30 \end{cases} \qquad (6)$$

where C_{mean} is the mean air concentration, x is the distance from the crest along the chute slope, L_i is the black water length from spillway crest to inception point, and y_i is the flow depth at the point of inception.

There is also a gradually varied flow region before the fully developed flow in which the following relation proposed by Chanson (1993) is used [10].

$$\frac{1}{(1-C_e)^2} Ln\left(\frac{1-C_{mean}}{C_e - C_{mean}}\right) - \frac{1}{(1-C_e)(1-C_{mean})} = k_0 s' + K_0 \qquad (7)$$

Where,

$$K_0 = \frac{1}{1-C_e}\left[\frac{1}{1-C_e} Ln\left(\frac{1-C_*}{C_e - C_*}\right) - \frac{1}{1-C_*}\right]$$

$$k_0 = \frac{u_r d_* \cos\phi}{q_w}$$

In which $s' = (S - S_*)/d_*$ and d_*, S_* and C_* are the flow depth at a reference position, the distance of reference position from the crest is measured along the chute, and the mean air concentration at the reference position, respectively. S is the distance from the crest measured along the chute, ϕ is the chute angle, and u_r is the upward vertical velocity of the air bubbles. This relation is obtained by solving the air phase continuity equation assuming that the mean air concentration reaches the equivalent mean air concentration value for fully developed flow region calculated by the empirical relation $C_e = 0.9\sin\phi$.

The following relations have been used for defining the inception point distance from the crest along the chute.

Chanson (1994) [11]:

$$\frac{L_i}{K} = 9.719(\sin\phi)^{0.796} F_h^{0.713} \qquad (8)$$

Chamani (1997) [12]:

$$\frac{L_i}{K} = 8.0 F_i^{0.858} \tag{9}$$

Boes & Minor (2002) [13]:

$$L_i = \frac{5.90 h_c^{6/5}}{(\sin\phi)^{7/5} s^{1/5}} \tag{10}$$

where, h_c is the critical depth, $K = s.\cos\phi$, $F_h = q / (g \sin\phi\ K^3)^{1/2}$, $F_i = q/(g.(s/l).K^3)^{1/2}$, $F_s = q/(g\ s^3)^{1/2}$, l and s are the step length and height, respectively and ϕ is the chute angle.

The following relations have been derived for defining the mixture flow depth at the point of inception.

Chanson (1994) [11]:

$$\frac{y_i}{K} = \frac{0.4034}{(\sin\phi)^{0.04}} F_h^{0.592} \tag{11}$$

Boes & Minor (2002) derived [13]:

$$y_i = \frac{0.40 s^{0.10} h_c^{0.90}}{(\sin\phi)^{0.30}} \tag{12}$$

where, h_c is the critical depth, $F_h = q / (g\sin\phi\ K^3)^{1/2}$ and ϕ is the chute angle.

Air concentration profiles, compared with an air bubble diffusion model proposed by Chanson (2000) [14], are expressed by:

$$C(y) = 1 - \tanh^2\left(K' - \frac{y}{2D'h_{90}}\right) \tag{13}$$

To define K' and D', the following relationships have been fit to experimental data:

$$K' = 0.729 C_{mean}^{-0.9932}$$

$$D' = 3.4558 C_{mean}^{3} - 2.2006 C_{mean}^{2} + 1.1059 C_{mean} - 0.0117$$

IV. Modeling Results

The numerical simulation results have been compared with those obtained from the experimental model study on the two-phase skimming flow down a stepped chute conducted at the laboratory of Hydraulics, Hydrology and Glaciology (VAW) of the Swiss Federal Institute of technology (ETH), Zurich [8]. The experiments have been conducted in a prismatic rectangular channel of width 0.5 m and length 5.7 m. The bottom angle $\phi = 30^\circ$ and the step height s=46.2mm have been used for comparison (Fig.1).

Three modeling strategies are presented in terms of flow depth and velocity as well as air concentration for skimming flow over a laboratory model of stepped spillway [6].

The measurements for the flow parameters (velocity profile at *x=3.8m* and *z=2.19m*) are reported for a unit width discharge of $q=0.13175\ m^2/s$ and Froude Number of *Fr*=4 (upstream velocity and depth of 2.74m/s and *0.048m*, respectively). The position of the measurements is located in the fully developed flow zone of the spillway for the above mentioned discharge.

The measurements for the air concentration distribution are reported for a unit width discharge of $q=0.049\ m^2/s$ and Froude Number of *Fr*=4 (upstream velocity and depth of *1.98m/s* and *0.025m*, respectively). For comparison of the computed air concentrations with the experimental measurements, three stations are used (Fig. 1). The positions of these stations are tabulated below. Note that , the stations 1 and 2 are located in gradually varied flow zone of the spillway, while the station 3 is located in the fully developed flow zone.

Table 1: vertical distances of the stations measured from the crest, $Z_i = (z - z_i) / h_c$

Station	Zi	z (m)
1	-0.5	0.43
2	0.9	0.52
3	41.3	3.06

A. Computation of Flow Parameters

The flow field parameters are computed by development of depth averaged flow solver version of *NASIR* software which solves SWE (modified for inclined slope) using cell vertex finite volume formulation for unstructured overlapping control volumes. The original software using finite volume method for solution of the modified shallow water equations for a coordinate system with an axis tangent to the slope direction (x') and another axis in transversal horizontal direction (y), was developed for flow simulation over steep sloped chutes with smooth bottom surface [1,2].

The depth and velocity values are depth-averaged values computed on a triangular unstructured mesh using the finite volume method. The equations are converted to discrete form using the overlapping cell vertex method.

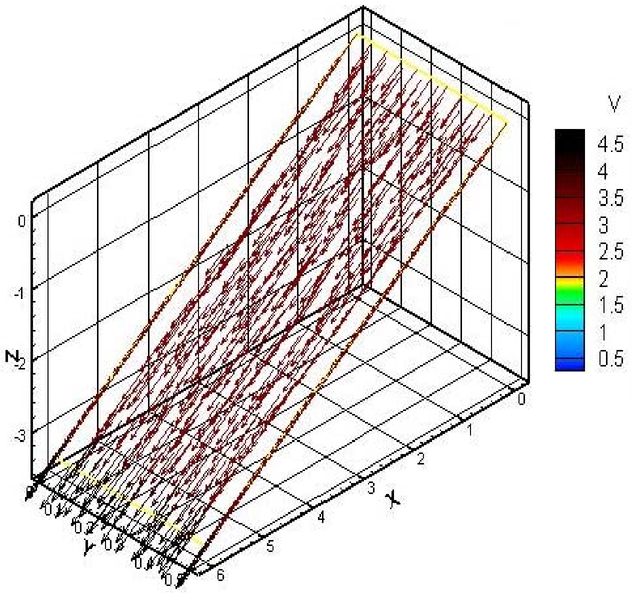

Fig. 2 Velocity vectors computed by *NASIR* depth averaged flow solver on sloping meshed surface

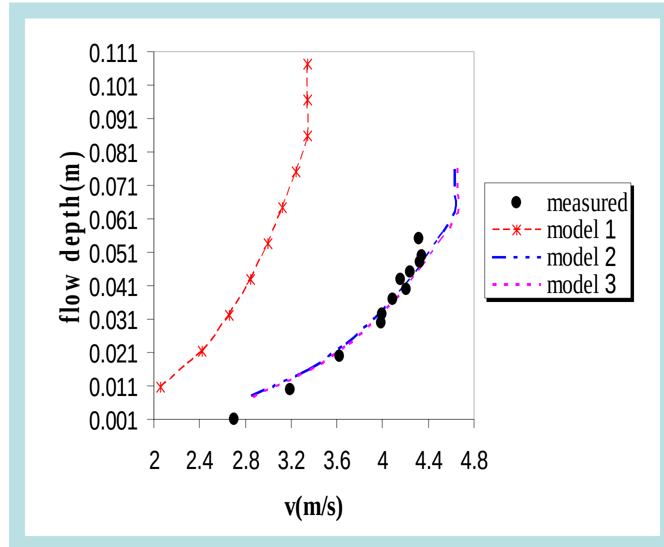

Fig. 3: Velocity profiles normal to the sloping virtual skimming flow bed using Chanson relation for inception point [11] and Matos relation for the mean air concentration [9]

For the numerical modeling of the problem, free slip boundary conditions in wall boundaries are applied by imposing zero normal velocity. At the boundary, supercritical inflow condition is imposed by enforcing depth and velocity components. The flow depth and velocity values imposed at the inflow boundary are *0.063 m* and *0.91 m/s*, respectively. The outflow boundary condition is considered free from implementation of any variables.

B. Effect of Mean Air Concentration Flow Parameters

In this section, the two relations reported in this paper for the mean air concentration in the skimming flow [15] and [6], for the fully developed skimming flow over stepped spillways are compared, and their effects on the formation of skimming flow depth and velocity as well as the air concentration distribution are numerically investigated.

In order to provide similar conditions for the use of two mean air concentration relations, certain relations for inception point distance and depth are used for both cases. Here, the relations for inception point distance and depth are applied [11].

It should be noted that, since the station of the laboratory measurements chosen for the assessment of the numerical model results is considered far from the air inception point (in fully developed part of the flow domain), the choice of relation for the location of the inception point of air entrainment and the flow depth at the inception point, have minor effect on the flow parameters (depth and velocity) computed via three modeling strategies in the fully developed flow region, (Fig. 3 and Fig. 4).

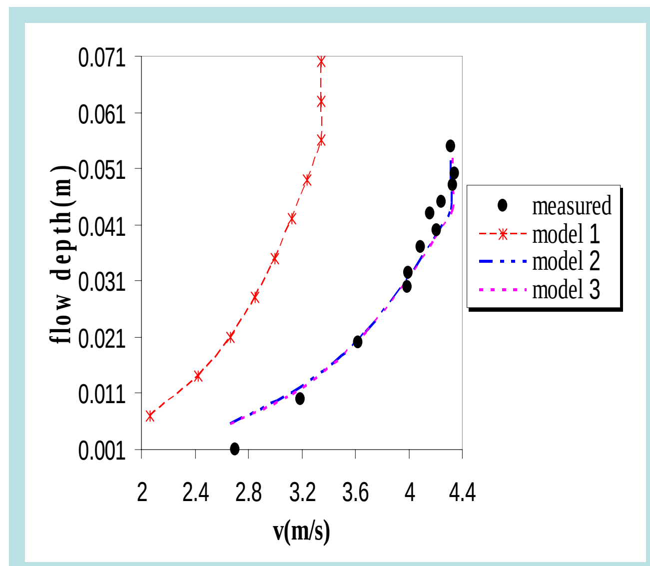

Fig. 4: Velocity profiles normal to the skimming flow virtual bed using Chanson relation for inception point location [11], Frizell et. al. relation for mean air concentration [6].

The errors in computing velocity parameters using the inception point distance relation proposed by Chanson [11] are tabulated below. As can be seen the errors of the first modeling strategy is considerably larger than the two other modeling strategies for both relations of mean air concentration.

In addition, there are minor differences between the results of the second and third modeling strategies, particularly for the Matos relation [9]. However the results obtained from by application of the mean air concentration relation suggested by Frizell et. al. [6] associates with considerably small value of error in computed flow variables.

Table 2: Error of computed mean velocity, using Chanson relation for the inception point distance [11].

Mean air concentration relation	Model 1	Model 2	Model 3
Frizell et al. [6]	22.9%	0.4%	0.2%
Matos [15]	22.9%	6.7%	7.4%

Table 3: Error of computed depth, using Chanson relation for the inception point distance [11].

Mean air concentration relation	Model 1	Model 2	Model 3
Frizell et al. [6]	27.3%	0.4%	0.5%
Matos [15]	95.1%	42.9%	42.4%

In order to compare the computed air concentrations with the reported laboratory measurements, the computed air concentration profiles, using the expression derived by Chanson [14] for the fully developed zone of the flow domain (station 3) are plotted using the mean concentrations computed by three modeling strategies (Fig. 5 and Fig. 6).

From the above tables and figures, it can be concluded that the relation proposed by Frizell et al. for mean air concentration [6] provides better results. This is the case not only for the air concentration distribution, but also for the flow depth and velocity in the fully developed region of the skimming flow over the stepped spillways.

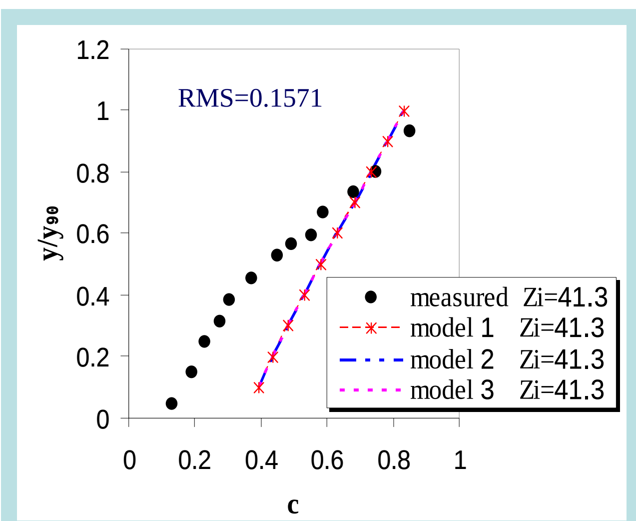

Fig. 5: Air concentration profiles normal to the skimming flow virtual bed at three stations, using Chanson relation for inception point location [11] and Matos relation for the mean air concentration [9].

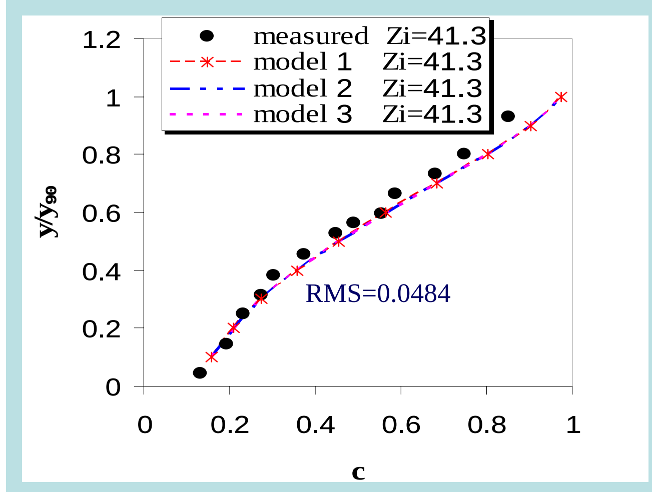

Fig. 6: Air concentration profiles normal to the sloping skimming flow virtual bed at three stations, using Chanson relation for inception point location [11] and Frizell et al. relation for the mean air concentration [6].

Therefore in the rest of paper the relation of Frizell et. al. [6] will be used for the computation of aerated flow parameters in fully developed part of the skimming flow over stepped spillway (using the three modeling strategies).

C. Air Inception Point Flow Depth

In this section two relations, reported in the literature for the flow depth at air inception point for the skimming flow over the stepped spillways proposed by Chanson [11] and Boes & Minor [13] are compared. The results of the computations show that both relations produce a unique value of *0.026m* for the flow condition of upstream unit width discharge of $q=0.049\ m^2/s$ and Froude Number of $Fr=4$ (velocity and depth of *1.98m/s* and *0.025m*, respectively). This is the case for all three modeling strategies. The laboratory observation for the inception point depth is reported as *0.028m*.

Therefore, it can be stated that there is no major differences in choosing any of the two relations mentioned in this paper.

D. Air Inception Point Distance from the Spillway Crest

Having chosen the proper relation for the air concentration distribution, the one proposed by Frizell et. al. [6], the effects of the relations proposed for the air inception point distance from the spillway crest are investigated in this section.

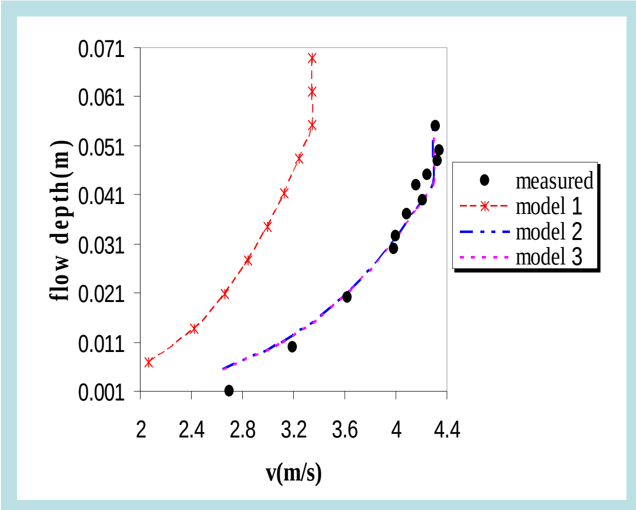

Fig. 7: Velocity profiles normal to skimming flow virtual bed using Chamani relation for inception point distance [12]

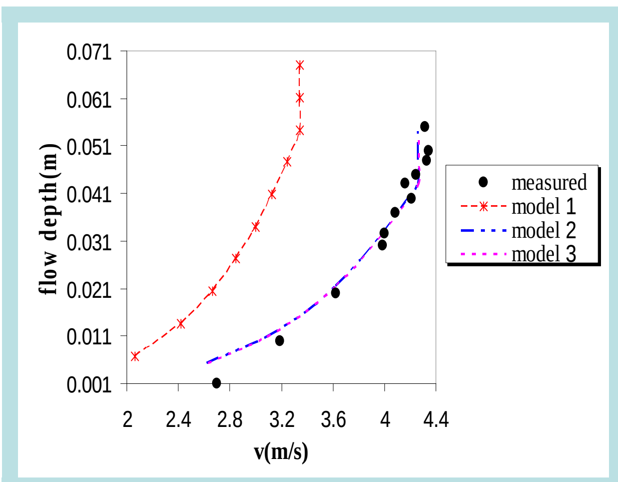

Fig. 8: Velocity profiles normal to skimming flow virtual bed using Boes & Minor relation for inception point distance [13]

As it can be seen the above figures are very similar to the velocity profiles computed, using the air inception point distance proposed by Chanson (Fig. 4). The calculated errors for the velocity profiles computed (by three modeling strategies) using various relations for air inception point distance from the crest of stepped spillway are tabulated in the following tables.

It can be seen that, there is a considerable constant error in the mean velocity results obtained from the first modeling strategy (post-processing of the air concentration on the final results of water flow computations). Therefore, the mean velocity results of the model 1 are not acceptable due to major differences with the laboratory measurements.

It is interesting to note that, the error in the computed flow depths is a different story. The error of the computed depth is not constant due to the effect of the mean air concentration. However, the results of the model 1 are not acceptable due to major differences with the laboratory measurements.

Table 4: Error of computed mean velocity, using Frizell et al. relation for mean air concentration in fully developed region [6].

Inception point distance relation	Model 1	Model 2	Model 3
Chanson [11]	22.9%	0.4%	0.2%
Chamani [12]	22.9%	1.1%	0.9%
Boes&Minor [13]	22.9%	1.8%	1.6%

Table 5: Error of computed depth, using Frizell et al. relation for mean air concentration in fully developed region [6].

Inception point distance relation	Model 1	Model 2	Model 3
Chanson [11]	27.3%	0.4%	0.5 %
Chamani [12]	25.3%	1.3%	1.3%
Boes&Minor [13]	23.6%	1.8%	2.0%

Table 6: RMS of computed velocity, using Frizell et al. relation for mean air concentration in fully developed region [6]

Inception point distance relation	Model 2	Model 3	Error
Chanson [11]	0.0812	0.0792	2.53%
Chamani [12]	0.0903	0.0878	2.85%
Boes&Minor [13]	0.1023	0.0993	3.02%

From the tabulated errors of the computed mean velocities, it can be concluded that the results of the third model coincide with less errors in comparison with the results of the second model. While the table of the errors of the computed depth using various relations for air inception point presents inverse condition.

Therefore in order to choose the best modeling strategy it is better to use a combined criterion in terms of velocity profile, in which, both velocity and depth can be compared with the laboratory measurements. Following table presents the comparison of the results of two modeling strategies for various air inception point relations.

From the table 6 it can be concluded that, for the second and third modeling strategies, there are some differences on the results produced by application of three relations utilized for computation of air inception point distance. As it can be seen the third modeling provides 2.5~3.0% improvement on the results.

From the air inception relation point of view, the relations proposed by Chanson [11] and Chamani [12] produce similar results, while the result computed using the air inception point distance derived by Boes & Minor [13] encounters more error in comparison with using two other relations.

E. Air Concentration Profile

The vertical distances of computed air inception point distances from the stepped spillway crest and the errors for various air inception point relations are compared with the laboratory measurements in the following table.

Although there are not major differences between the errors in z_i of three stations for any of the air inception point relations, the plot of air concentration profile presents different results computed in two gradually varied flow and fully developed flow regions (Fig. 9 to Fig. 11)

Table 7: Computed inception point distance (Experimental measurement $z_i = 0.4m$)

		0.4	0.5	3.0
Chanson [11]	z (m)	0.233	0.234	0.234
	Error	41.5%	41.8%	41.8%
Chamani [12]	z (m)	0.364	0.366	0.366
	Error	9.0%	8.5%	8.5%
Boes&Minor [13]	z (m)	0.522	0.524	0.524
	Error	31.0%	30.5%	30.5%

In the gradually varied flow region application of the relations proposed by Chanson [11] and Chamani [12] produce acceptable results, while the relation suggested by Boes & Minor [13] fails to produce realistic results due to calculation of excessive value for the air inception point location.

On the other hand, in the fully developed flow region, the relation derived by Boes & Minor [13] provides better computed air concentration profiles, while the computed results obtained by application of the air inception point proposed by Chamani [12] and Chanson [11] present slightly weaker computational results. However, in general all three relations provide good agreement with the laboratory measurements.

Although the relation for air inception point distance proposed by Chamani [12] presents the least error with the experimental observations (Table 7), the two relations for air inception point distance suggested by Chanson and Chamani [12] provide proper means for computing air concentration profiles in both gradually varied and fully developed skimming flow regions of stepped spillways (Fig. 9 and Fig 10).

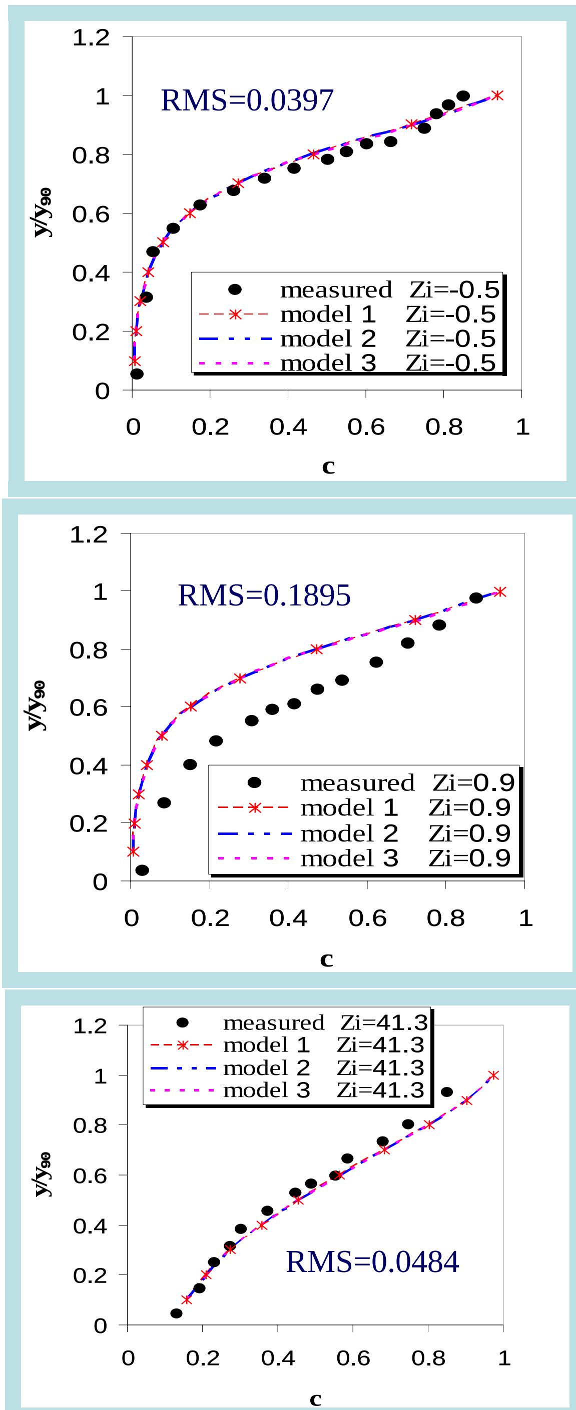

Fig. 9: Air concentration profiles normal to skimming flow virtual bed at three stations, using Chanson relation for air inception point distance [11]

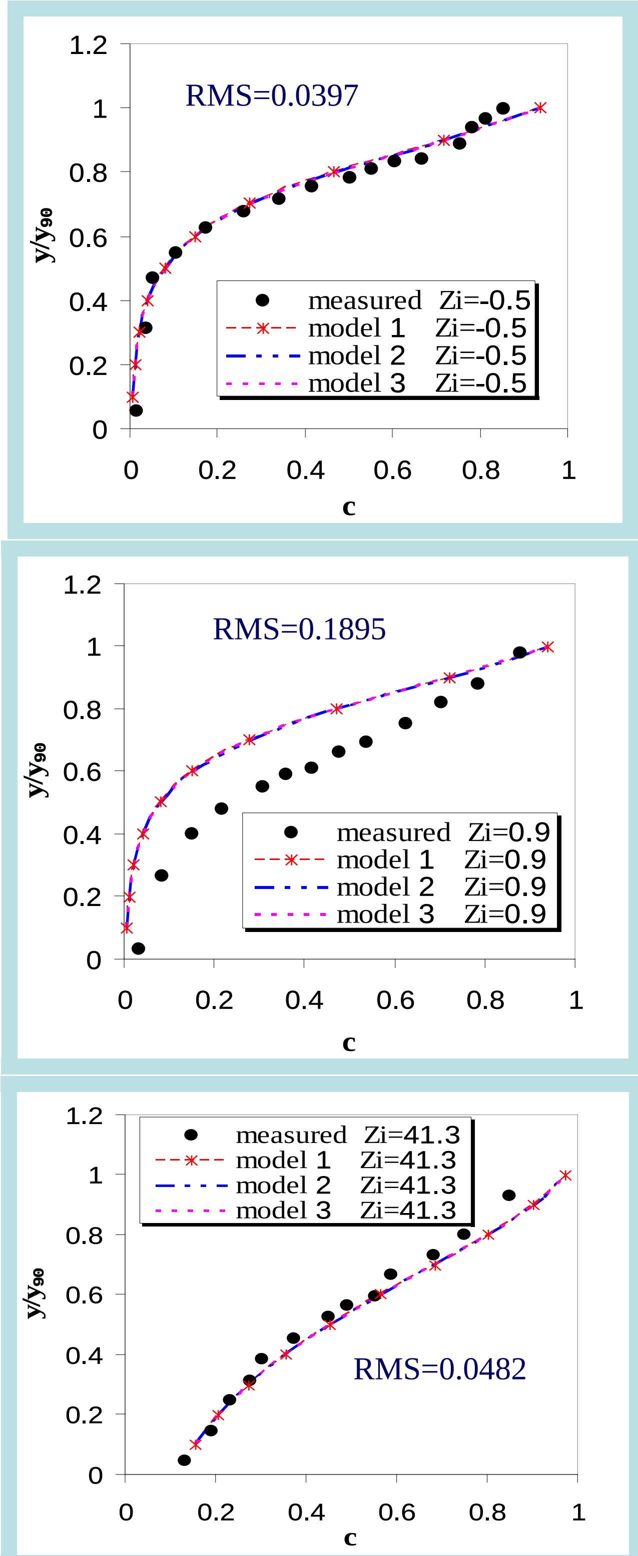

Fig. 10: Air concentration profiles normal to skimming flow virtual bed at three stations, using Chamani relation for air inception point distance [12]

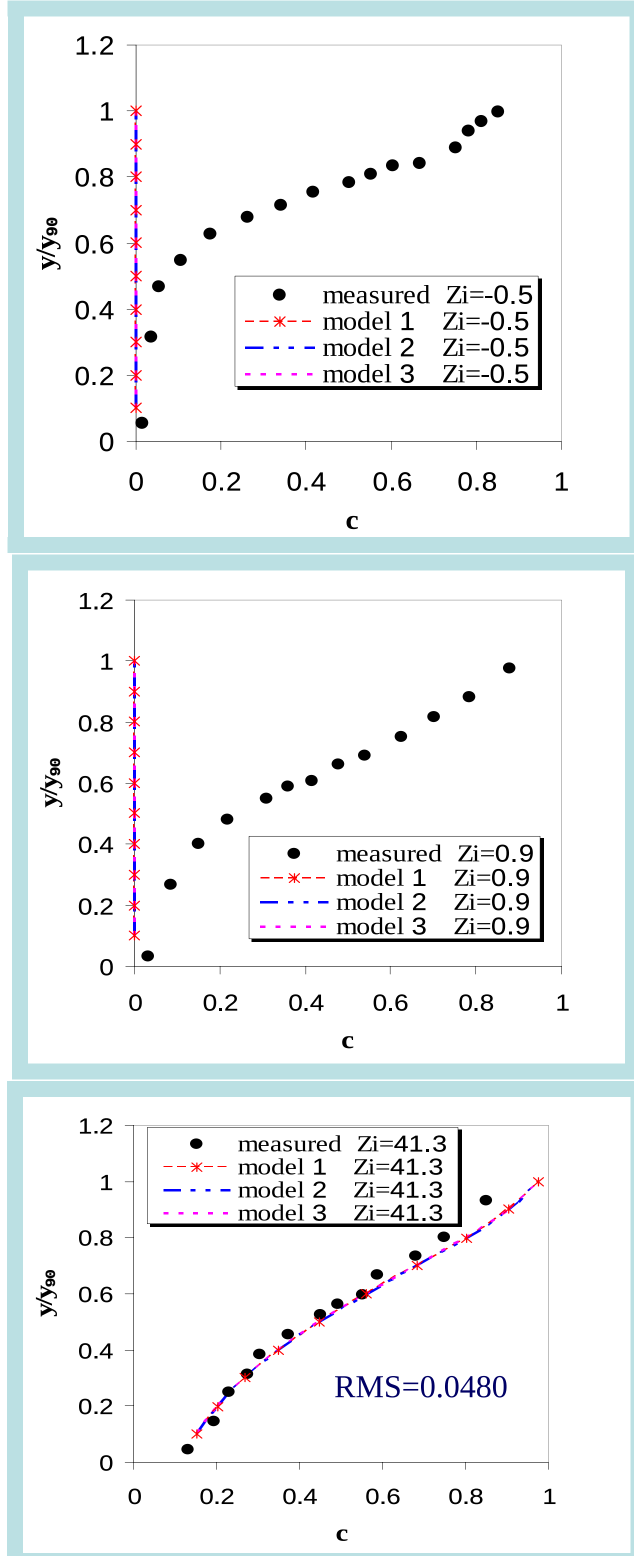

Fig. 11: Air concentration profiles normal to skimming flow virtual bed at three stations, using Boes & Minor relation for inception point distance [13].

Note that, the relation proposed by Chanson [10] for computation of air concentration in gradually varied flow region provides realistic results if the position of air inception point is computed accurately. The relation suggested by Boes & Minor [13] produces excessive air inception distance and computing excessive distance disturbs the air concentration computations in the gradually varied flow region.

V. Concluding Remarks

In order to investigate the effects of air concentration parameters on computing skimming flow parameters over stepped spillways, the numerical analysis of aerated flow have been carried out, using three modeling strategies. In the first modeling strategy, the air concentration parameters are computed using the final results of the numerical solution of depth averaged water flow equations (SWE adopted for flow over steep slope surface). In the second modeling strategy, the mean air concentration distribution is computed at every time step of the previously described numerical solution and its effects on reduction of bed friction and flow depth bulking are considered in the formation of flow field. In the third modeling strategy, the effects of changes in air-water mixture density (by means of a term in the two equations of motions) are added to the second modeling strategy. The effects of various relations for computing air concentration in skimming flow over stepped spillways on the quality of the results of three modeling strategies are examined in this paper. The qualities of the computed results are assessed through comparison with the laboratory measurements reported in the literature.

The numerical investigations using empirical formulas required for computation of air concentration distribution ended up with following conclusions:

- There is no difference between the computed air inception point depth using relations suggested by Chanson [11] and Boes & Minor [13].
- The relation proposed by Chanson (1993a) for computation of air concentration in gradually varied flow region of skimming flow provides realistic results, if the position of air inception point is computed accurately. Computing excessive distance disturbs the air concentration computations in the gradually varied flow region of the skimming flow.
- Among the various relations for defining inception point distance from the stepped spillway crest, the one proposed by Chamani [12] provides more accurate results. Although the relation proposed by Chanson [12] results in shorter air inception distance, its effect on computed parameters of aerated flow is very similar to the relation suggested by Chamani [12]. The relation suggested by Boes & Minor [13] produces excessive air inception distance, and therefore, would disturb the air concentration computations in the gradually varied flow region of the skimming flow.
- The relation proposed by Frizell et al. [6] for defining mean air concentration in the fully developed skimming flow provides better results in comparison with the relation proposed by Matos [9].

From the three modeling strategies (for the numerical analysis of aerated skimming flow on stepped spillways) point of view, the following conclusions can be stated.

- The first modeling strategy produces poor aerated flow parameters (depth, velocity and air concentration)
- The accuracies of the computed results of the second and third modeling strategies are pretty similar. However, the third modeling strategy produces slightly more accurate results with the expense of additional numerical solution work load for computation of an extra term in each of the two equations of motions.

The quality of the computational results presented in this paper proves the efficiency and accuracy of the developed finite volume solver of the sloping SWE (2D Free Surface Flow Solver version of *NASIR* software) to simulate the aerated skimming flow over stepped spillways.

References

[1] S.R. Sabbagh-Yazdi, *Spillway Flow Modeling by Finite Volume Solution of Slopping Depth Averaged Equations on Triangular Mesh*; *Application to KAROUN-4 Spillway*, 10th WSEAS International Conference on Applied Mathematics, Dallas (Texas), USA, 2006.

[2] S.R. Sabbagh-Yazdi, M. Zounemat and N.E. Mastorakis, *Velocity Profile over Spillway by Finite Volume Solution of Slopping Depth Averaged Flow*, WSEAS Journal of Applied and Theoretical Mechanics, Issue 3, Vol.2, , 2007, pp.85-94.

[3] S.R.Sabbagh-Yazdi, R. Safahieh and N.E. Mastorakis, *Post-Processing of Air Entrainment on NASIR Flow Solver Results for Skimming Flow over Stepped Chutes*, 9th WSEAS Int.Conf. on Automatic Control, Modeling & Simulation (ACMOS'07) , Istanbul, Turkey, 2007.

[4] S.R. Sabbagh-Yazdi and R. Safahieh, *Computing Velocity and Air Concentration Profiles using Depth Averaged Solution of Skimming Flow on Stepped Spillways*, 32th Congress of IAHR, Venice, Italy, 2007.

[5] S.R. Sabbagh-Yazdi and R.Safahieh, *Numrical Modeling of Aerated Flow over Stepped Spillways using NASIR Software*, 3th National Congress of Civil Engineering, Tabriz, Iran, 2007, (Farsi).

[6] K.H. Frizell, J. Matos, A.N. Pinheiro, *Design of Concrete Stepped Overlay Protection for Embankment Dams*; © Swets & Zeitlinger, Netherlands, 2000.

[7] M. Boes and H. Hager, *Two-Phase Flow Characteristics of Stepped Spillways*, J. Hydraulic Eng., Vol.129, No.9, 2003, pp. 671-679.

[8] M. Boes, H. Hager, *Hydraulic Design of Stepped Spillways*, J. Hydraulic Eng., Vol.129, No.9, pp. 671-679, 2003.

[9] J. Matos, J. *Hydraulic Design of Stepped Spillways Over RCC Dams*, *Hydraulics of Stepped Spillways*; © Swets & Zeitlinger, Netherlands, 2000.

[10] H. Chanson, *Self-Aerated Flows on Chutes and Spillways*, J. Hydraulic Eng., ASCE, Vol.119, No.2, 1993, pp. 220-243.

[11] H. Chanson, *State of the Art of the Hydraulic Design of Stepped Chute Spillways*, Hydropower Dams J. , 1994, pp. 33-42.

[12] M.R. Chamani, *Skimming Flow in a large Model of a Stepped Spillway*, Thesis for the Degree of Doctor of Philosophy in Water Resources Engineering, 1997.

[13] R. Boes, and H.E. Minor, *Hydraulic Design of Stepped Spillways for RCC Dams*, Hydropower Dams, Vol.9, No.3, 2002, pp. 87-91.

[14] H. Chanson, *Discussion of 'Characteristics of Skimming Flow Over Stepped Spillways'* by M. R. Chamani and N. Rajaratnam, J. Hydraulic Eng., Vol.126, No.11, 2000, pp. 862-865.

[15] J. Matos, Sanchez M., Quintela A., Dolz, J. Air Entrainment and Safety against Cavitation Damage in Spillways Over RCC Dams, Hydraulics of Stepped Spillways, Balkema Publishers; © Swets & Zeitlinger, Netherlands, 2000.